



Stress-associated scattering attenuation and intrinsic attenuation from ultrasonic measurements

Li-Yun Fu, Yan Zhang, Wei Wei, Bing Zhang and Zhenxing Yao

Institute of Geology and Geophysics, Chinese Academy of Sciences

19 Beitucheng Xi Rd 100029 Beijing, China

E-mail lfu@mail.iggcas.ac.cn;

SUMMARY

Acoustic attenuation has been proved to be an indicator of stress changes in solid structures. Acoustic coda, as a superposition of incoherent scattered waves, reflects small-scale random heterogeneities in solids. Acoustic coda attenuation, as a combination of intrinsic attenuation and scattering attenuation, contains information on stress changes as a result of changes in the physical state of small-scale heterogeneous structures. Based on the ultrasonic measurements of a rock sample with intra-grain pores and fractures under different pore-pressure induced effective stresses, we compute the stress-associated coda attenuation quality factors Q_{PC} and Q_{SC} as a function of frequencies. Based on the digital heterogeneous cores of the sample, the experimental results are validated and corrected with numerical results by the finite-difference simulation of Biot's poroelastic equations and the Monte Carlo simulation of multiple scatterings, respectively. The quality factors characterize its scale dependence of scattering attenuation on stress variations in rocks. We compare them with the intrinsic attenuation quality factors Q_P and Q_S calculated by the spectral ratio method and BISQ model, respectively, from ultrasonic measurements. Comparisons demonstrate that the scattering attenuation is much stronger, particularly when ultrasonic wavelengths are comparable to the scale of pores and grains. The intrinsic and coda attenuations versus increasing effective stresses present quite different nonlinear features, where Q_{PC} and Q_{SC} show a greater sensitivity to pore pressure than Q_P and Q_S .

Key words: reverse time migration; data storage; Nyquist theorem; compression algorithm; finite-difference

INTRODUCTION

Inferring stress changes from seismic waves has long been an important topic during the past several decades, confused by the complex relationship between static and dynamic elastic moduli (e.g., Simmons and Brace, 1965; Ciccotti and Mulargia, 2004). Generally, the manner in which a dynamic wave catches information on static stress is associated with variations in the physical state of materials induced by stress changes. Against the large-scale heterogeneous structures, the small-scale random heterogeneities, which could be measured by scattering attenuation, may be more sensitive to stress changes of the Earth's interior as a result of changes in the physical state of materials. Coda waves, recorded as the tail portion of a seismogram, have been proved to be generated by scattering at the small-scale random heterogeneities in the lithosphere (Aki,

1969; Wu, 1982; Fehler, 1982; Sato and Fehler, 1998). Coda attenuation has been commonly measured in the frequency range of 1 to 30 Hz. It is a useful seismological tool to estimate the strength of random heterogeneity in the lithosphere, but whether there is a direct relationship with tectonic stress changes is as yet uncertain.

Wave scattering in short wavelengths has long been interesting to geophysicists, where ultrasonic waves interact with small-scale random heterogeneities on a scale of micrometres. However, ultrasonic wave propagation in heterogeneous porous cores is an extremely complex process where scattering effects by individual pores and grains are generally neglected. Laboratory measurements have shown that the attenuation level predicted by the combined effect of various mechanisms (e.g., the mesoscopic-loss, viscoelastic, and squirt-flow mechanisms) underestimates the measured level of dispersion and attenuation in rocks (e.g., Dvorkin et al., 1995; Mavko et al., 1998; Arntsen and Carcione, 2001). Ultrasonic scattering attenuation may be dominant, particularly when wavelengths are comparable to the scale of pores and grains where the scattering effect will be significant (Wu, 1989). Ultrasonic scattering attenuation by small-scale random heterogeneities in porous cores can be measured by ultrasonic coda waves, i.e., the tail portion of an ultrasonic wavetrain, which is often ignored in ultrasonic measurements, possibly because of the sample-size limitation of experiments, the contamination of boundary reflections, the unknown heterogeneity in rocks, and the complexity of received waveforms (Stacey and Gladwin, 1981).

Based on the ultrasonic measurements of a rock sample with intra-grain pores and fractures under different pore-pressure induced effective stresses, we investigate the stress-associated coda attenuation by the Sato weak scattering model. Based on the digital heterogeneous cores of the sample, the experimental results are validated and corrected with numerical results by the finite-difference simulation of Biot's poroelastic equations and the Monte Carlo simulation of multiple scatterings, respectively. The coda quality factor characterizes its scale dependence of scattering attenuation on stress variations in rocks. Comparisons of the intrinsic (by the spectral ratio method and BISQ model) and scattering attenuations induced by stress variations show both the attenuations increase with decreasing effective stress, but with quite different nonlinear features. The scattering attenuation shows a greater sensitivity to pore-pressure variations.

ROCK PROPERTIES AND MEASUREMENTS

The rock sample shown in Figure 1 (left panel) is a high porosity (19.7%), moderate permeability (43.5 mD) massive sandstone. It comprises moderately sorted, sub-angular to sub-

rounded quartz grains (0.1-0.3 mm diameter) in point contact with one another. Pore size is variable, ranging from about 0.1 mm up to about 0.4 mm. The minor clays and glauconite that are present generally reside in pores and most grain boundaries are direct contacts between rigid framework grains. Testing is performed under ambient pressure conditions along the stress path with a constant confining pressure of 65 MPa while the pore pressure increases incrementally from 5 to 60 MPa, and then returning to 5 MPa. Ultrasonic measurements comprise full waveform recordings of both transmitted P -waves and S -waves at nominal centre frequencies of 600 kHz.

Wave propagation in random heterogeneous media is classified into different heterogeneous scales, depending upon the parameters $k\alpha$ and kL , in which k is the wavenumber, α is the correlation length (a characteristic scale length of heterogeneity), and L is the travel distance of waves. Such a subtle characteristic length is generally controlled by the averaging sizes of grains and pores within the heterogeneous core. Based on the present experimental data, the S -wave velocity decreases from about 2462 m/s down to about 2232 m/s as pore pressure grows from 5 to 60 MPa, and coda attenuation is calculated for 0.4–0.8 MHz at 0.1 MHz spacing. The resulting distribution of $k\alpha$ and kL is confined to the hatched zone as shown in Figure 1(right panel), indicating a medium heterogeneity scale of the rock sample.

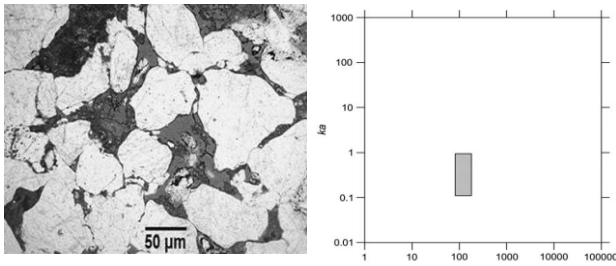


Figure 1. Close-up of the sandstone sample (left panel), showing microstructures with various sizes of grains and pores, and its ka - kL scattering distribution (right panel) for the present experiment, indicating a medium heterogeneity scale of the rock sample.

INTRINSIC ATTENUATION

We measure Q_P and Q_S by the pulse transmission technique and spectral ratio method (Toksoz et al., 1979) with the assumption of constant quality factors over the bandwidth (0.4–1MHz). The method is based on a comparison between pulse shapes observed in a reference material (Aluminum) and in the sandstone sample of the same geometry. Quality factors can be obtained from least-squares fits to the slope of the natural log of the ratio of spectral amplitudes of pulse shapes in rock sample and reference material. Plots of Q_P and Q_S versus effective stress for the sample are shown in Figure 2, where a steep decrease in Q_P and Q_S is indicative of the opening microcracks as pore pressure varies from 5 to 60 MPa (with a constant confining pressure 65 MPa). The faster decreasing rate of Q_P than Q_S suggests that the attenuation of P waves is more sensitive to the relative motion between the framework and pore fluid than S waves. It should be noted that the quality factor values measured may also include a scattering loss term, in addition to the intrinsic losses. Therefore, the quality factor values observed possibly underestimates of the true intrinsic attenuation.

The spectral ratio method generally requires the ratio of diameter/length of rock samples to be equal or greater than 1.0 and the diameter of rock samples to be equal or greater than

10λ (λ is the wavelength). The present sample and experiment far cannot meet the requirement, possibly causing large errors. In an attempt to determine the intrinsic loss mechanisms producing the observed Q values more accurately, the BISQ model (Dvorkin and Nur, 1993) is examined in this study. The resulting BISQ quality factors versus effective stress for the sample are shown in Figure 3 with compared to other types of quality factors. We see that the absolute values observed for Q_P are consistent with the values predicted from BISQ attenuation theory. This may be coincidental as other evidence suggests that frictional losses in the interstitial clay may be a significant factor.

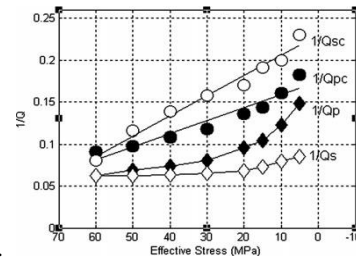


Figure 2. Plots of intrinsic attenuation, Q_P and Q_S , and coda attenuation, Q_{PC} and Q_{SC} , versus effective stress.

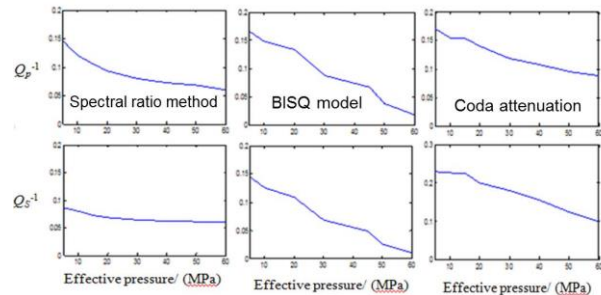


Figure 3. Plots of BISQ quality factors versus effective stress with compared to other types of quality factors.

SCATTERING ATTENUATION

The ultrasonic coda as a continuous waveform in the tail portion of an ultrasonic wavetrain, as shown in Figure 4a and 4b for P and S waves, respectively, is composed of a superposition of incoherent scattered waves by microscale heterogeneities in porous cores. It has been used to measure scattering attenuation in the ultrasonic frequency range (Guo and Fu, 2007; Guo et al., 2009) by the Sato weak scattering model with the assumption that the distribution of random scatterers is homogeneous and isotropic (leading to spherical radiation and isotropic scattering). The calculation of Q_{PC} and Q_{SC} from the slope of a straight line fitting the mean-square amplitudes of coda waves is shown in Figure 4c and 4d for P and S waves, respectively, along with the plot of the coda window with time.

The resulting Q_{PC} and Q_{SC} under a number of different stress conditions are shown in Figure 2 with compared to Q_P and Q_S . We see that coda attenuation appears a great sensitivity to stress changes. The intrinsic and coda attenuations increase as effective stress decreases. Both are close at high effective stresses, but with increasing pore pressure (effective stress decreases), the coda waves attenuate faster than the direct P and S waves. In fact, increased pore pressure would compress the pore lining clays adjacent to framework grain contacts, resulting in increased stiffness for normal compression and

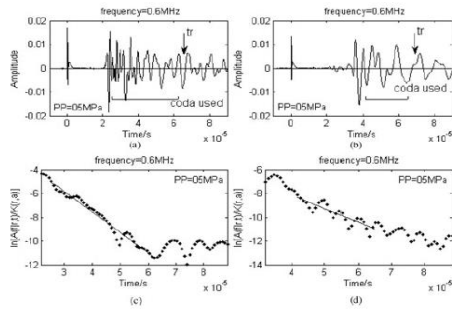


Figure 4. Unfiltered P -wave (a) and S -wave (b) data traces with coda windows. The functions of coda energy density versus lapse time t along with the best least-square fits of selected P -coda (c) and S -coda (d) windows filtered at a central frequency of 600 kHz.

decreased resistance to tangential displacements (Dvorkin et al.1991). It consequently causes a faster and stronger attenuation of P waves. The population of grains in contacts appears to decrease in a linear fashion since the reduction in stiffness, and therefore the attenuation of coda obviously shows a strong linear correlation. Comparing intrinsic attenuation to coda attenuation, we can clearly see that the scattering of S -wave is much stronger and more stable than P wave, this may due to the shorter wavelength of S waves.

The window length is made short to reduce contamination of multiple reflections from the side ends and the reverberations between the sample surfaces. Although the contamination cannot be absolutely excluded from the earlier portion of waveforms, its effect on the linear regression of slope results is small for the calculation of Q_{PC} and Q_{SC} . Too short of a coda window length, however, may reduce the accuracy of calculation significantly. It is difficult to extract pure coda waves from ultrasonic measurements. Numerical simulations with absorbing boundary for ultrasonic wave propagation in digital heterogeneous cores are used to offer decisive information on how the boundary reflections affect the P - and S -codas in laboratory experiments. Two different schemes of simulation are used for this purpose in this study.

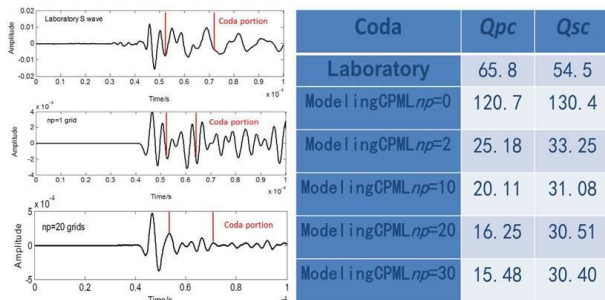


Figure 5. Comparisons of experimental (top trace) and numerical (the rest two traces in the left panel) records for ultrasonic S -waves with the selected coda portions. The calculated Q_{PC} and Q_{SC} are listed in the right panel with the numerical simulation under different CPML thicknesses.

Gurevich (1996) suggested that all numerical simulations based on complex rheological models should be compared to an equivalent elastic model. This invokes comparisons of poroelastic effects between experimental and numerical data. A rotated staggered-grid finite-difference method of Biot poroelastic equations with unsplit convolutional perfectly matched layer (CPML) absorbing boundary (Zhang et al., 2010) is used to simulate ultrasonic wave propagation in digital heterogeneous cores (Zhang et al., 2014). Based on the characteristics of the true porous core picture, we can extract a

2D model surrounded by CPML layers, where white color indicates the quartz grains and black color indicates the clays reside in pores. Oil is assumed to fill in the whole background so that it is double phases in each point of the model, either it is oil with quartz grains or it is oil with clay grains. We use the same source with a centre frequency of 600 kHz as used in the laboratory ultrasonic experiment. We take the grid intervals $\Delta x = \Delta z = 0.00005$ m. The CPML absorbing layer varies from thin (with numerous boundary reflections) to thick (with few boundary reflections). The radial and vertical components of the stress and velocity are recorded at one receiver located at the bottom of the model to analyse the effect of the boundary reflections on transmitted elastic waves.

Figure 5 compares numerical and experimental records for ultrasonic S -waves and the calculated Q_{PC} and Q_{SC} with the numerical simulation under different CPML thicknesses. We see that the boundary reflection is so strong at a thin CPML layer that significantly contaminates the tail portion of records, and thus makes the codas Q_{PC} and Q_{SC} considerably larger than the experimental values. The decay of boundary reflections is fast as increasing the CPML thickness. The resulting codas Q_{PC} and Q_{SC} reduce to a normal level after $np=20$. These numerical examples indicate that boundary reflections contaminate coda waves seriously, which can increase the passage of energy in the medium, leading to much larger value of coda quality factor, and decrease the scattering attenuation.

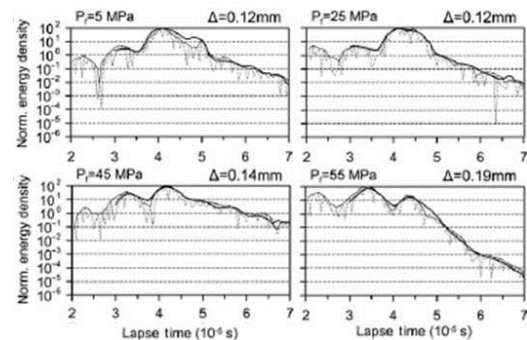


Figure 6. Comparisons of the observed (thin lines) and synthesized (thick lines) S -coda envelopes under different pore pressures (5, 25, 45, and 55 MPa) for the time window from 3×10^{-5} to 6×10^{-5} s. The numerical S -coda envelopes are optimally synthesized by the fourth-order Monte Carlo method to fit the observational S -wave energy densities (dotted lines).

Considering the complexity of ultrasonic coda waveforms measured from finite-size rock samples in laboratory experiments, the Monte Carlo simulation is employed to synthesize ultrasonic envelopes for the 3D sample under study, which act by incorporating the effect of multiple scatterings and boundary reflections on coda waves. The simulation is restricted to acoustic wave equations because the only S -wave excitation is studied here. S -coda quality factor Q_{SC} is defined to give an approximate estimation for S coda attenuation. The Monte-Carlo simulation represents the propagation of S -wave energy by the movement of many particles. The energy density for each order of scattering wave is computed separately. The multiple-scattering effects are obtained by summing over all orders of energy densities. The characteristic scale length of heterogeneity is a crucial parameter to control scattering effects particularly when comparable to wavelengths. Unlike the traditional applications to the lithosphere, the Monte-Carlo simulation for a laboratory rock sample with a detailed structure of grains and pores from thin sections of the sample

enables us to incorporate the characteristic scale length of heterogeneity into the Monte-Carlo simulation for improvement of the algorithm in the implementation. The optimal simulation parameters are estimated by minimizing the residual between the observed and synthesized envelopes.

As shown in Figure 6, the comparisons of envelopes with good agreement between the observed (thin lines) and numerical (thick lines) ultrasonic data for most pore pressures, especially in the coda time window during which the maximum deviation of the residual is less than 5%. Figure 7 compares the intrinsic (by spectral ratio method), the Monte-Carlo single-scattering, and the Monte-Carlo multiple-scattering attenuation quality factors plotted against effective stress. It should be noted that both the Monte-Carlo single-scattering and multiple-scattering attenuation quality factors contain the effect of boundary reflections as taking place in laboratory measurements. We see that the single-scattering model significantly underestimates ultrasonic S -coda attenuation. Unlike the linear correlation shown in Figure 2 estimated by the Sato single-scattering model without considering the effect of boundary reflections, the scale dependence of ultrasonic S -coda attenuation on effective stress shows a strong-nonlinear correlation.

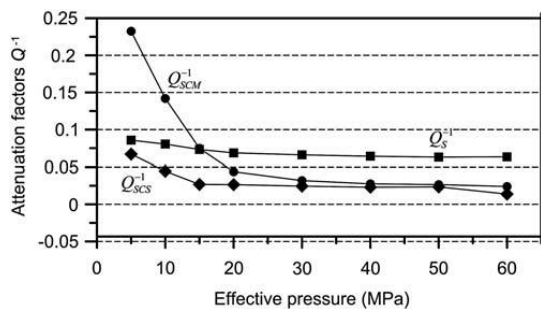


Figure 7. Comparisons of the S -wave intrinsic (Q_S by spectral ratio method), the Monte-Carlo single-scattering S -coda (Q_{SCS}), and the Monte-Carlo multiple-scattering S -coda (Q_{SCM}) attenuation quality factors versus effective stress, with the simulation considering the effect of boundary reflections.

ACKNOWLEDGMENTS

We gratefully thank Laboratory of High-Temperature and High-Pressure Geodynamics, Institute of Geology and Geophysics, Chinese Academy of Sciences for great help in preparing experimental data. This research was supported by the National Natural Science Foundation of China (Grant No. 40925013).

REFERENCES

- Aki, K., 1969. Analysis of seismic coda of local earthquakes as scattered waves: *Journal of Geophysical Research* 74, 615–631.
- Arntsen, B., Carcione, J.M., 2001. Numerical simulation of the Biot slow wave in water-saturated Nivelsteiner Sandstone: *Geophysics* 66, 890–896.
- Ciccotti, M., Mulargia, F., 2004. Differences between static and dynamic elastic moduli of a typical seismogenic rock: *Geophysical Journal International* 157, 474–477.
- Dvorkin, J.P., Nur, A.M., 1995. Elasticity of high-porosity sandstones: Theory for two north sea datasets: *Society of Exploration Geophysicists*. Document ID: 1995–0890. (1995 SEG Annual Meeting, October 8 - 13, Houston, Texas)
- Dvorkin, J., Mavko, G., Nur, A., 1991. The effect of cementation on the elastic properties of granular material: *Mechanics of Materials* 12, 207–217.
- Fehler, M., 1982. Interaction of seismic waves with a viscous liquid layer: *Bulletin of the Seismological Society of America* 72, 55–72.
- Gurevich, B., 1996. On “ Wave propagation in heterogeneous, porous media: a velocity - stress, finite difference method ” by Dai, N., Vafidis, A., Kanasevich, E.R. (March - April 1995 *Geophysics*, 327 - 340). *Geophysics* 61, 1230 - 1232.
- Guo, M.Q., Fu, L.Y., 2007. Stress associated coda attenuation from ultrasonic waveform measurements: *Geophysical Research Letters* 34, L09307.
- Guo, M.Q., Fu, L.Y., Ba, J., 2009. Comparison of stress-associated coda attenuation and intrinsic attenuation from ultrasonic measurements: *Geophysical Journal International* 178, 447–456.
- Mavko, G., Mukerji, T., Dvorkin, J., 1998. *The rock physics handbook: Tools for seismic analysis of porous media*: Cambridge University Press.
- Sato, H., Fehler, M., 1998. *Seismic Wave Propagation and Scattering in the Heterogeneous Earth*: Springer-Verlag, New York.
- Stacey, G.P., Gladwin, M.T., 1981. Rock mass characterization by velocity and Q measurement with ultrasonics, in *Anelasticity in the Earth: Geodynamics Series* 4, 78–82, American Geophysical Union, Boulder, Co.
- Simmons, G., Brace, W.F., 1965. Comparison of static and dynamic measurements of compressibility of rocks: *Geophysics* 70, 649–656.
- Toksoz, M.N., Johnson, D.H., Timur, A., 1979. Attenuation of seismic waves in dry and saturated rocks, I: laboratory measurements: *Geophysics* 44, 681–690.
- Wei, W., Fu, L.Y., 2014. Monte Carlo simulation of stress-associated scattering attenuation from laboratory ultrasonic measurements. *Bull. Seismol. Soc. Am.* 104, 931–943.
- Wu, R.S., 1982. Attenuation of short period seismic waves due to scattering: *Geophysical Research Letters* 9, 9–12.
- Wu, R.S., 1989. Seismic wave scattering, in *The Encyclopedia of Solid Earth Geophysics*: edited by James, D., pp. 1166–1187, Van Nostrand Reinhold, New York.
- Zhang, L.X., Fu, L.Y., Pei, Z.L., 2010. Finite difference modeling of Biot’s poroelastic equations with unsplit convolutional PML and rotated staggered grid: *Chinese Journal of Geophysics (abstract in English)* 53, 2470–2483.
- Zhang Y., Fu L.Y., Zhang L.X., Wei W., Guan, X.Z., 2014. Finite difference modeling of ultrasonic propagation (coda waves) in digital porous cores with un-split convolutional PML and rotated staggered grid: *Journal of Applied Geophysics* 104, 75–89.